Organization of telomeric nucleosomes: atomic force microscopy imaging and theoretical modeling

Rosella Mechelli[a], Claudio Anselmi[b], Stefano Cacchione[a], Pasquale De Santis[b], Maria Savino[a,c,*]

[a]*Dipartimento di Genetica e Biologia Molecolare, Università di Roma "La Sapienza", Fondazione Istituto Pasteur-Fondazione Cenci Bolognetti, Piazzale A. Moro 5, I-00185 Rome, Italy*
[b]*Dipartimento di Chimica, Università di Roma "La Sapienza", P.le A. Moro 5, I-00185 Rome, Italy*
[c]*Istituto di Biologia e Patologia Molecolare, CNR, P.le A. Moro 5, I-00185 Rome, Italy*

Abstract Telomeric chromatin has peculiar features with respect to bulk chromatin, which are not fully clarified to date. Nucleosomal arrays, reconstituted on fragments of human telomeric DNA and on tandemly repeated tetramers of 5S rDNA, have been investigated at single-molecule level by atomic force microscopy and Monte Carlo simulations. A satisfactory correlation emerges between experimental and theoretical internucleosomal distance distributions. However, in the case of telomeric nucleosomal arrays containing two nucleosomes, we found significant differences. Our results show that sequence features of DNA are significant in the basic chromatin organization, but are not the only determinant.
© 2004 Federation of European Biochemical Societies. Published by Elsevier B.V. All rights reserved.

1. Introduction

The organization of telomeric chromatin is characterized by peculiar features with respect to bulk chromatin, such as the unusually short nucleosome spacing [1] and the reduced stoichiometric ratio between the linker histone and the histone octamer [2]. Telomeric DNAs are straight, since they consist mostly of 6–8 base pairs (bp) tandem repeats, therefore out of phase with respect to the B-DNA periodicity [3]. Due to their peculiar DNA sequence feature, we previously found that telomeric nucleosomes are characterized by the highest free energy of nucleosome formation with respect to all biological and synthetic DNAs studied so far [4]. Furthermore, we found that telomeric nucleosomes occupy isoenergetic positions having the periodicity of the telomere repeat [5]. Both nucleosome features (thermodynamic stability and lack of rotationally phased positioning) can be satisfactorily predicted from their DNA sequences by the theoretical method we have recently developed [6,7]. On the contrary, 5S rDNA represents a well-known nucleosome-positioning sequence, characterized

by a nucleosome main position embedded in a set of rotationally phased minor positions [8].

In this paper, we study the sequence-dependent basic features of telomeric chromatin organization by atomic force microscopy (AFM) imaging. We have taken advantage of AFM capability to investigate a complex system at single-molecule level. Nucleosomal arrays were reconstituted on human telomeric DNA fragments containing $(TTAGGG)_{135}$ repeats (H-Tel$_{135}$) and compared with those reconstituted on tetramers of 5S rDNA (5S-208$_4$), having the same length. The internucleosomal distances of subsaturated nucleosomal arrays, containing two, three and four nucleosomes, respectively, were measured. The important role of DNA sequence in the organization of nucleosomal arrays emerges from the satisfactory correlation between the experimental and theoretical distance distributions, the latter obtained by Monte Carlo simulations. However, in the case of telomeric arrays containing two nucleosomes, we found significant differences between the experimental behavior and the theoretical prediction. This finding suggests that factors, different from sequence-dependent nucleosome positioning, could be involved in the chromatin basic organization.

2. Materials and methods

2.1. DNA fragments

The 5S-208$_4$ was prepared by partially digesting the plasmid pPOL208.12 with *Ava*I [9], containing 12 copies of 5S rDNA from *Lytechinus variegatus* (a gift from R. Sendra). The DNA fragments corresponding to the 5S-208$_4$ were gel extracted and cloned in the *Eco*RV site of pSTBlue1 after filling in protruding ends. 5S-208$_4$ was purified by gel extraction after plasmid digestion with *Hin*dIII and *Bam*HI.

The H-Tel$_{135}$ was excised from the plasmid pSXneo [10] (a gift from H. Cook) by *Bam*HI and *Bgl*II double digestion and purified by gel extraction.

2.2. Histone octamer preparation

H1–H5 stripped chromatin was prepared from chicken erythrocytes nuclei. Purified histone octamers were obtained from polynucleosomes by hydroxyapatite chromatography, as previously described [4].

2.3. Nucleosomal arrays reconstitution

Oligonucleosomes were reconstituted onto H-Tel$_{135}$ and 5S-208$_4$ by salt dilution method at room temperature [11], using a 1:1 weight ratio of DNA to purified histone octamer. Samples at 1.0 M NaCl were incubated for 30 min at 25 °C and then diluted to 0.1 M NaCl by adding 10 mM Tris–HCl (pH 7.5) by five dilution steps (at 20 min

---

intervals). The final nucleosome concentration is about 20 mg/ml. All samples were fixed by dialysis with 0.1% glutaraldehyde in 10 mM Tris–HCl (pH 7.5); 1 mM EDTA for 3 h at 4 °C. Excess of glutaraldehyde was removed by a final dialysis for 16 h against 10 mM Tris–HCl (pH 7.5), 1 mM EDTA at 4 °C.

2.4. Sample preparation for AFM imaging

Immediately prior to loading the sample on mica surface, reconstituted oligonucleosomes solutions were approximately diluted 10-fold on ice. 20 µl of the sample (DNA concentration 24 µg/ml) in 10 mM Tris–HCl (pH 7.5) and 1 mM EDTA was applied on spermidine-treated mica (SPD-mica), obtained according to Sato et al. [12], for 3 min, rinsed with deionized water and dried with nitrogen.

2.5. AFM imaging

AFM images were taken with a MultiMode SPM instrument Nanoscope Digital III A, equipped with E-scanner (Digital Instruments Inc., Santa Barbara, CA), operating in tapping mode using canonical sharp silicon tips. AFM images of nucleosomal arrays were converted from Nanoscope format into TIF files and the internucleosomal (center-to-center) distance measurements were made using SigmaScan Pro software (SPSS Inc., Chicago, IL). Internucleosomal distances of molecules containing two, three, and four nucleosomes, respectively, were measured. For each class, about 60–200 molecules were examined in each of the three independent experiments. Distance distributions were reported as histograms with bin size of 7.5 nm (about 22 bp), a value representative of AFM resolution power. Errors on bin heights were evaluated as the square root of the number of counts [13].

2.6. Theoretical modeling

Nucleosome distribution along DNA sequences was evaluated by means of Monte Carlo simulations. Starting DNA structures were generated by evaluating the local intrinsic curvature and twisting angles by means of Webdna program [14,15]. Nucleosomes were generated imposing the correct curvature on 145 bp DNA tracts, which form a superhelix with a 4.18 nm radius and a 2.39 nm pitch, in agreement with the crystallographic data [16,17]. Analogously, the nucleosomal DNA periodicity was set equal to 10.2 bp/turn. Linker entry-exit angle was imposed to be 90°, but with non-crossing linker DNAs, as seen in electron microscopy images [18]. From 2 up to 4 nucleosomes were generated along the sequence. Nucleosome positioning and the relative free energy were evaluated as aforementioned [6,7,14].

Short-range interactions between nucleosomes were parameterized using the Gay–Berne potential for oblate ellipsoids [19–21]. Different configurations of nucleosomal arrays were generated following the Metropolis-Monte Carlo method [22]: first, nucleosomes are randomly moved from their original positions; then the change in energy is calculated. If $\Delta E < 0$, then we allow the nucleosomes in the new positions. If $\Delta E > 0$, we allow the change with a probability $\exp(-\Delta E/RT)$. By this method, we generated a canonical ensemble of nucleosomal arrays.

Internucleosomal distances were measured on different statistical thermodynamic ensembles of 5880 DNA molecules with 2, 3 and 4 nucleosomes, respectively. To mimic the effects of thermal fluctuations, following Kratky and Porod [23], distances were multiplied by $[2X(1 - X(1 - \exp(-1/X)))]^{1/2}$, with $X = P/nl$, where $P = 45$ nm and $l = 0.34$ nm are the DNA persistence length and the helix rise, respectively. Finally, n is the DNA linker length.
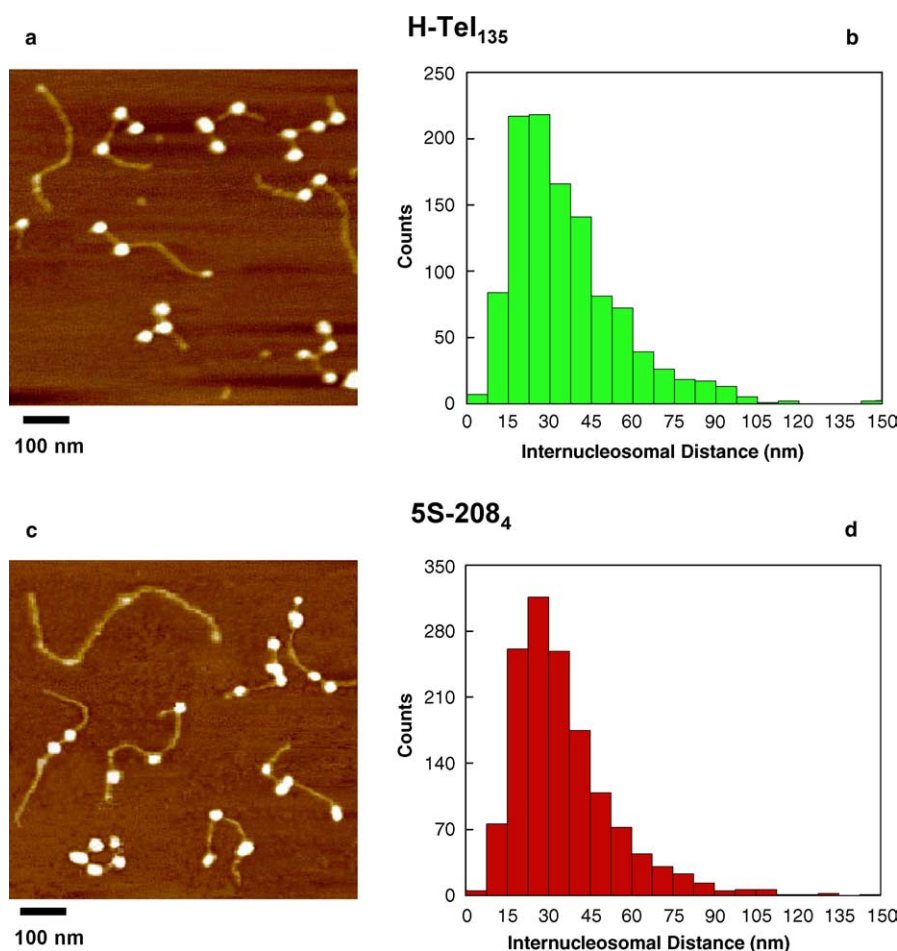

Fig. 1. AFM images of nucleosomal arrays and the relative histograms of internucleosomal distance. (a,b) H-Tel$_{135}$. (c,d) 5S-208$_4$. Bars represent 100 nm.

3. Results

3.1. AFM imaging and internucleosomal distance distributions

AFM images were quantitatively characterized by the measurements of the internucleosomal distances, since this parameter is directly connected with nucleosome positioning. Nucleosomal arrays reconstituted on H-Tel$_{135}$ and 5S-208$_4$ were deposited on SPD-mica [12] after glutaraldehyde fixation, in order that the nucleosome positions on the mica surface are the same than in solution.

Fig. 1 shows typical AFM images of nucleosomal arrays reconstituted on H-Tel$_{135}$ (Fig. 1(a)) and on 5S-208$_4$ (Fig. 1(c)), as well as the distributions of the internucleosomal distances relative to the whole set of molecules with 2, 3 and 4 nucleosomes (Figs. 1(b) and (d)). The two histograms are similar, although the distribution appears to be slightly broader in the case of H-Tel$_{135}$. Therefore, the different nucleosome positioning strength of the two DNA sequences

cannot be usefully analyzed at this level (combined histograms). Since AFM permits to investigate nucleosomal arrays at single-molecule level, data from experiments were clustered into different subsets depending on the number of nucleosomes present in the arrays, i.e., all the arrays with two nucleosomes in one subset, those with three nucleosomes in another one and finally those with four nucleosomes in yet another. This permits to test for nucleosome number dependence in the positioning features.

Fig. 2 reports the internucleosomal distance distributions, distinguished on the basis of the number of nucleosomes. In the case of arrays with two nucleosomes, the distributions are markedly different between the two DNAs. As for H-Tel$_{135}$, a maximum is clearly evident at 30 nm (Fig. 2(a)) corresponding to the preferential spacing of about 55 bp (taking into account the nucleosome width equal to 11 nm). In the case of 5S-208$_4$, the histogram is characterized by a bimodal distribution with two maxima at 30 and 65 nm, corresponding to about 55 and 160 bp, respectively (Fig. 2(b)).

The internucleosomal distance distributions for molecules having 3 and 4 nucleosomes are similar in both the cases: the more represented values are 30 and 20 nm for H-Tel$_{135}$ (Figs. 2(c) and (e)), 35 and 30 nm for 5S-208$_4$, respectively (Figs. 2(d) and (f)). As expected, increasing the nucleosome number, the average internucleosomal distance decreases. However, given a certain number of nucleosomes, the more frequent distance is always shorter for telomeric arrays. This is more noticeable in the case of four nucleosomes. It can be related to the unusual short nucleosomal repeat of the telomeric chromatin, which allows nucleosomes to come closer to each other, without being penalized by unfavorable nucleosome positioning.

3.2. Theoretical evaluation of internucleosomal distances frequency distributions

We recently developed a theoretical method, based on sequence-dependent DNA curvature and flexibility, which allows the quantitative prediction of nucleosome positioning [6,7]. Fig. 3 reports the corresponding profiles for H-Tel$_{135}$ and 5S-208$_4$, respectively. The one relative to H-Tel$_{135}$ is characterized
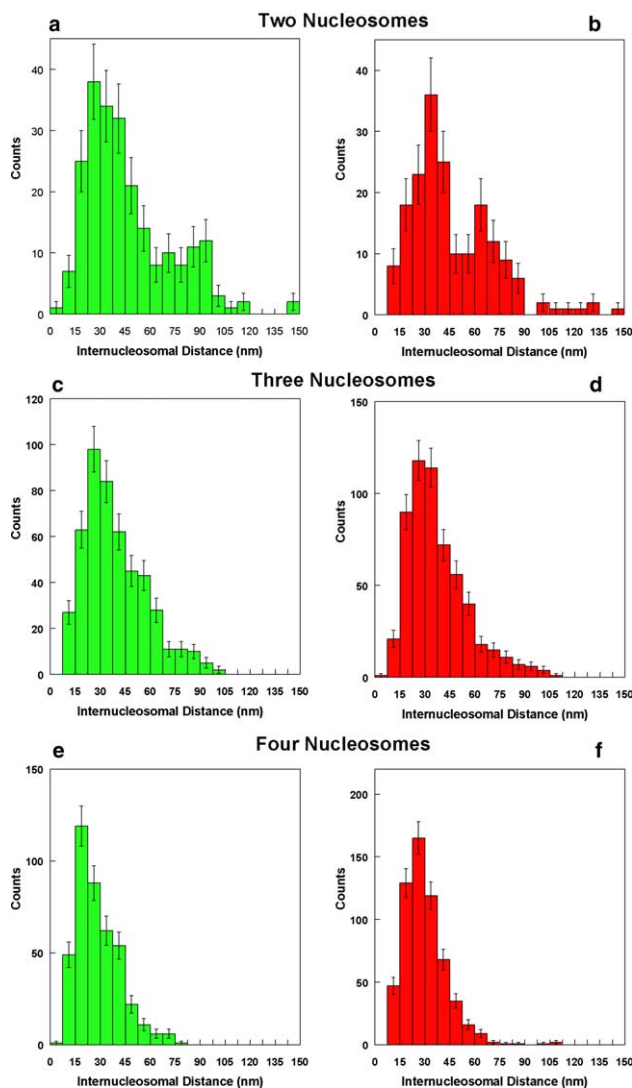

Fig. 2. Internucleosomal distance distribution histograms referring to H-Tel$_{135}$ (left) and to 5S-208$_4$ (right). (a,b) Two nucleosomes. (c,d) Three nucleosomes. (e,f) Four nucleosomes. Error bars reflect the statistical uncertainty on the bin height and are calculated as the square root of the number of counts [13].
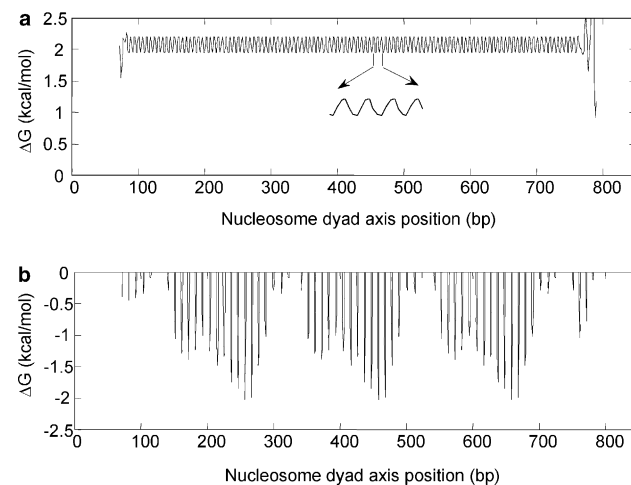

Fig. 3. Theoretical nucleosome dyad axis positioning on H-Tel$_{135}$ (a) and on 5S-208$_4$ (b). The minima correspond to the energetically most favored nucleosome dyad axis positions. The inset is to put in evidence that the nucleosome positioning profile has the same periodicity (6 bp) as that of the human telomeric DNA repeat (TTAGGG).

by multiple isoenergetic positions for the nucleosome dyad axis, spaced every 6 bp (Fig. 3(a)), in agreement with the previous experimental results [5]. On the contrary, the theoretical profile relative to 5S-208$_4$ DNA (Fig. 3(b)) shows three free-energy minima, each consisting of a number of quasi equivalent energy positions, rotationally oriented in phase with the B-DNA periodicity. It is worth noting that nucleosome positions on a multimer are not the mere reproduction of those found on the monomer, since new positions emerge from the head-to-tail regions. The theoretical sequence-dependent nucleosome positioning is the more important constraint adopted in Monte Carlo simulations (see Section 2) to discriminate between the nucleosomal distributions of the two studied DNAs on the basis of their sequences. The two other constraints, namely short-range nucleosome–nucleosome interactions, modeled by the Gay–Berne potential, and DNA

flexibility, following Porod and Kratky, are not sequence dependent and are equal between the two DNAs.

Monte Carlo simulations were performed by sorting the molecules in different classes, depending on the number of nucleosomes (as in the case of experimental data in Fig. 2), and collecting ensembles of about 5880 molecules for each class. Fig. 4 shows the comparison between the experimental and the theoretical internucleosomal distance distributions. Experimental data and theoretical predictions are, generally, in satisfactory agreement. A significant discrepancy is observed only for telomeric arrays containing two nucleosomes (Fig. 4(a)), where the experimental internucleosomal distance distribution (characterized by a maximum at 30 nm) is considerably narrower than the theoretical broad profile. In the corresponding case for 5S-208$_4$, both experimental and theoretical profiles are characterized by two maxima at about the same positions, although with different frequencies. These findings strongly suggest the involvement of determinants different from nucleosome positioning in the organization of subsaturated nucleosomal arrays. In addition, these parameters seem to be more important in the case of telomeres.

4. Discussion

Whereas the role of DNA sequence in nucleosome stability and positioning has been extensively studied, less is known about the relevance of sequence-dependent features in the assembly of nucleosomal arrays. Their properties have been often investigated using oligonucleosomes reconstituted on tandem repeats of 5S rDNA, a well-known strong nucleosome positioning sequence used as model system [24].

Despite its important role in chromosome building, telomeric nucleosome organization has not been fully clarified. This partially derives from the difficulty with analyzing telomeric polynucleosomal systems, which are characterized by the absence of positioning signals.

In this work, we have taken advantage of AFM ability to investigate the organization of nucleosomal arrays at single-molecule level and discriminate the level of saturation of the potential nucleosome binding sites. Telomeric nucleosomal arrays have been compared with those reconstituted on 5S rDNA tetramers with the same length. Similar internucleosomal distance distributions were obtained, except for those arrays which contain two nucleosomes. Whereas the profile relative to H-Tel$_{135}$ is characterized by a maximum at 30 nm, in the case of 5S-208$_4$, the internucleosomal distance distribution is bimodal with two maxima at 30 and 65 nm.

We have performed Monte Carlo simulations to connect the internucleosomal distance distributions to the sequence-dependent nucleosome positioning. The agreement between theoretical and experimental data is quite satisfactory, except in the case of telomeric arrays containing two nucleosomes (Fig. 4(a)). Since nucleosomes are positioned with equal probability every 6 bp (Fig. 3(a)) [5], the theoretical probability of having a certain internucleosomal distance is approximately proportional to the number of available configurations with two nucleosomal binding sites at that distance; this eventually results to be in inverse proportion to the distance itself. Therefore, the theoretical profile is characterized by a broad profile. On the contrary, the experimental distance distribution
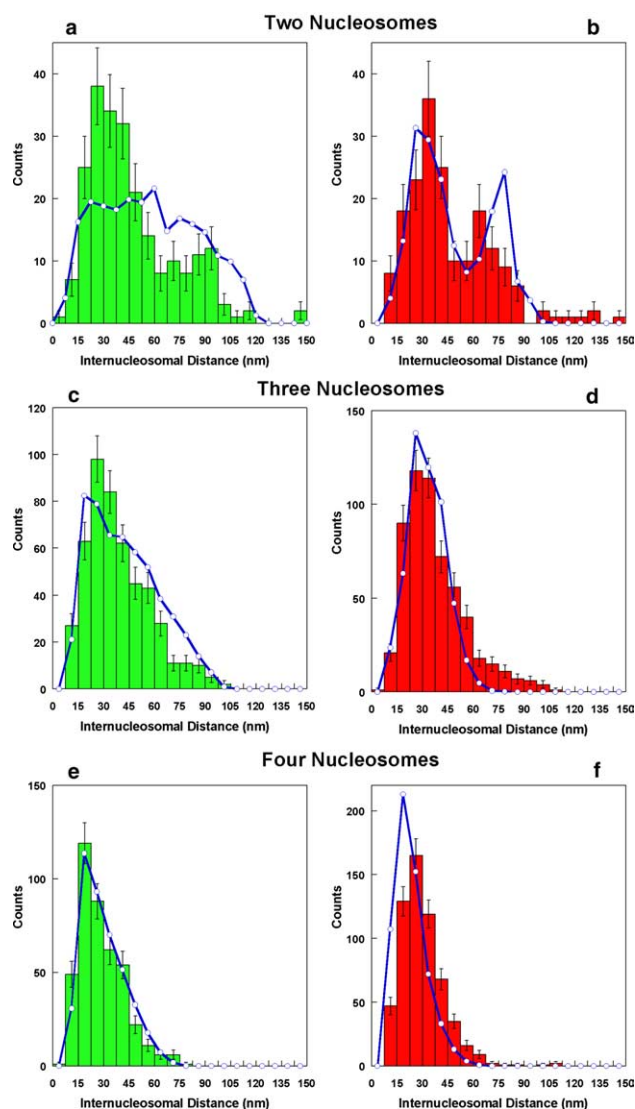

Fig. 4. Comparison between the experimental and the theoretical profiles of the internucleosomal distances referring to H-Tel$_{135}$ (left) and to 5S-208$_4$ (right). (a,b) Two nucleosomes. (c,d) Three nucleosomes. (e,f) Four nucleosomes. Error bars reflect the statistical uncertainty on the bin height and are calculated as the square root of the number of counts [13].

shows a narrower peak with a maximum at about 30 nm. This discrepancy suggests that sequence-dependent nucleosome positioning is not the only determinant in the assembly of nucleosomal arrays. As recently reported [16,25,26], interactions between adjacent nucleosomes due to the histone tails, which span about 20–30 bp, as well as DNA flexibility could be involved in determining the linker DNA length.

We suggest that, in our experiments, equilibration on mica does not influence the nucleosome positions on DNA, but opens the dinucleosome structure. As a result, the internucleosomal distances increase to about 55 bp. The main reason should be the stiffening of the adsorbed linker DNAs with respect to those in solution, due to the dimensional reduction of the DNA dynamics on the mica surface [27,28].

In the case of 5S-208$_4$ DNA arrays containing two nucleosomes, nucleosome positioning signals appear prevalent. Therefore, the role of internucleosomal interactions in non-saturated chromatin organization seems more important if strong positioning signals are lacking. Obviously, internucleosome interactions should be involved also in the organization of arrays containing three and four nucleosomes. However, in these cases, their influence is masked by the progressive filling of the potential nucleosome binding sites.

References

[1] Makarov, V.L., Lejnine, S., Bedoyan, J. and Langmore, J.P. (1993) Cell 73, 775–787.

[2] Bedoyan, J., Lejnine, S., Makarov, V.L. and Langmore, J.P. (1996) J. Biol. Chem. 271, 18485–18493.

[3] Rossetti, L., Cacchione, S., Fuà, M. and Savino, M. (1998) Biochemistry 37, 6727–6737.

[4] Cacchione, S., Cerone, M.A. and Savino, M. (1997) FEBS Lett. 400, 37–41.

[5] Filesi, I., Cacchione, S., De Santis, P., Rossetti, L. and Savino, M. (2000) Biophys. Chem. 83, 223–237.

[6] Anselmi, C., Bocchinfuso, G., De Santis, P., Savino, M. and Scipioni, A. (1999) J. Mol. Biol. 286, 1293–1301.

[7] Anselmi, C., Bocchinfuso, G., De Santis, P., Savino, M. and Scipioni, A. (2000) Biophys. J. 79, 601–613.

[8] Meersseman, G., Pennings, S. and Bradbury, E.M. (1991) J. Mol. Biol. 220, 89–100.

[9] Georgel, P., Demler, C., Terpening, M.R., Paule, K.E. and van Holde, K. (1993) J. Biol. Chem. 265, 19839–19847.

[10] Podgornaya, O.I., Bugaeva, E.A., Voronin, A.P., Gilson, E. and Mitchell, A.R. (2000) Mol. Reprod. Dev. 57, 16–25.

[11] Cacchione, S., Rodrìguez, J.L., Mechelli, R., Franco, L. and Savino, M. (2003) Biophys. Chem. 104, 381–392.

[12] Sato, M.H., Ura, K., Hohmura, K.I., Tokumasu, F., Yoshimura, S.H., Hanaoka, F. and Takeyasu, K. (1999) FEBS Lett. 452, 267–271.

[13] Bevington, P.R. (1969) Data Reduction and Error Analysis for the Physical Sciences. McGraw-Hill Book Company Inc..

[14] http://archimede.chem.uniroma1.it/webdna/.

[15] Anselmi, C., De Santis, P., Paparcone, R., Savino, M. and Scipioni, A. (2002) Biophys. Chem. 95, 23–47.

[16] Luger, K., Mader, A.W., Richmond, R.K., Sargent, D.F. and Richmond, T.J. (1997) Nature 389, 251–260.

[17] Davey, C.A., Sargent, D.F., Luger, K., Mader, A.W. and Richmond, T.J. (2002) J. Mol. Biol. 319, 1097–1113.

[18] Hamiche, A., Schultz, P., Ramakrishnan, V., Oudet, P. and Prunell, A. (1996) J. Mol. Biol. 257, 30–42.

[19] Gay, J.G. and Berne, B.J. (1981) J. Chem. Phys. 74, 3316–3319.

[20] Wedemann, G. and Langowski, J. (2002) Biophys. J. 82, 2847–2859.

[21] Bešker, N., Anselmi, C., Paparcone, R., Scipioni, A., Savino, M. and De Santis, P. (2003) FEBS Lett. 554, 369–372.

[22] Metropolis, N., Rosenbluth, A.W., Rosenbluth, M.N., Teller, A.H. and Teller, E. (1953) J. Chem. Phys. 21, 1087–1092.

[23] Kratky, O. and Porod, G. (1949) Recl. Trav. Chim. Pays-Bas Belg. 68, 1106–1122.

[24] Yodh, J., Woodbury, N., Shlykhtenko, L., Lyubchenko, Y. and Lohr, D. (2002) Biochemistry 41, 3565–3574.

[25] Zheng, C. and Hayes, J.J. (2003) J. Biol. Chem. 278, 24217–24224.

[26] Wang, X., He, C., Moore, S.C. and Ausio, J. (2001) J. Biol. Chem. 276, 12764–12768.

[27] Rivetti, C., Walker, C. and Bustamante, C. (1998) J. Mol. Biol. 280, 41–59.

[28] Scipioni, A., Anselmi, C., Zuccheri, G., Samorì, B. and De Santis, P. (2002) Biophys. J. 83, 2408–2418.